RESEARCH PAPER

High-Temperature Deformation Behavior and Microstructural Evolution of Nb-10Hf-1Ti Alloy Produced by Vacuum Arc Melting

S. Ranjbar Motlagh[1], H. Momeni[2],*

* *h_momeni@mut.ac.ir*

[1] PhD of materials science and engineering, Faculty of Material & Manufacturing Technologies, Malek Ashtar University of Technology, Iran

[2] Assistant Professor, Faculty of Material & Manufacturing Technologies, Malek Ashtar University of Technology, Iran

Abstract: The present work deals with the hot deformation behavior of commercial Nb alloy C-103 and its microstructure evolution during uniaxial compression tests in the temperature range of 700-1100°C and the strain rate range of 0.001-0.4 s⁻¹. Strain rate sensitivity, calculated from the compression tests data, was almost constant and showed a negative value in the temperature range of 700-900°C but increased significantly beyond 900°C. Dynamic strain aging was found to have a predominant effect up to 900°C, beyond which dynamic recovery and oxidation influenced the compressive properties. The microstructure of the deformed samples showed indications of dynamic recrystallization within the high strain rate sensitivity domain and features of flow instability in the regime of low strain rate sensitivity. The 950–1000°C temperature range and strain rate range of 0.001-0.1 s⁻¹ were suggested as suitable hot deformation conditions. The constitutive equation was established to describe the alloy's flow behavior, and the average activation energy for plastic flow was calculated to be 267 kJ/mol.

Keywords: Niobium alloy, Hot deformation, Strain rate sensitivity, Dynamic recrystallization, Constitutive equation.

1. INTRODUCTION

Niobium and its alloys are used in several industries, including aerospace, nuclear, defence, electronics, and biology. These alloys have the lowest density (8.57 g/cm³) among all the refractory metals (Mo, Ta, W, and Rh) and exhibit a good combination of high-temperature strength, room-temperature ductility, and good weldability[1]. Alloying Nb with elements like Ti, Hf, and Zr significantly improves their high-temperature oxidation resistance. Of various Nb alloys, the Nb-Hf-Ti alloy system is widely used in high-temperature applications due to excellent physical, thermal, and mechanical properties up to 1300°C[2]. In this alloy system, C-103 with a nominal composition of Nb-10Hf-1Ti (%wt.) is used in lightweight space propulsion systems because of superior mechanical properties at all temperatures. Although considered a first-generation alloy, the succeeding Nb-1Zr, C-103, was developed to replace the weaker alloys and retain the desirable formability characteristics and welding properties [3].

Though several studies have been conducted on the deformation behavior and high-temperature mechanical properties of Nb and its alloys [4–9], most are confined to pure Nb and Nb-Zr alloys.

Sarkar et al. [10] They studied the hot deformation behavior of the Nb-1Zr-0.1C alloy and identified domains of hot workability by mapping the strain rate sensitivity. However, to the author's best knowledge, no systematic study on the hot deformation behavior of C-103 at different temperatures and strain rates exists. Only Panwar et al. [11] They studied dynamic strain aging of C-103 during tensile deformation in the temperature range of 600-1200°C and at a strain rate of 10^{-2} s⁻¹. Still, they did not investigate the effect of concurrent changes in strain rate and temperature on the thermomechanical behavior of C-103 alloy. Consequently, this investigation seeks to characterize the deformation response of the alloy across a spectrum of temperatures and strain rates to ascertain optimal hot working parameters.

2. EXPERIMENTAL PROCEDURES

The chemical composition was measured using the wet chemical method and inductively coupled plasma (ICP) mass spectroscopy. The ingot of the alloy was produced by the vacuum arc melting (VAR) method. It was remelted twice under vacuum conditions to obtain a homogenized melt. The production ingot was produced in the form of

H. Momeni et al.

a cylinder with a height of 40 cm and a diameter of 15 cm. The homogenizing process was carried out in a tube furnace at 1600°C for 3 h under an argon-protected atmosphere, and then the furnace cooled down to room temperature.

Cylindrical samples with a diameter of 8 mm and a height of 12 mm were cut using electrical discharge machining to perform uniaxial compression tests. Compression tests were carried out at temperatures of 700, 800, 900, 1000, and 1100°C and strain rates of 0.001, 0.01, 0.1, and 0.4 s⁻¹ according to ASTM E209. Since Nb alloys are sensitive to oxidation, all compression tests were carried out under a protected atmosphere. All the samples were preheated at the test temperature for 5 min before loading to ensure that the sample had reached the temperature. Graphite was used as a lubricant to reduce the friction between the sample and the machine. The compression tests were continued to a true strain of 0.6 to minimize the barrelling effect. The morphologies of the initial and milled powders and their microstructure were examined on a TSCAN–VEGA3 scanning electron microscopy (SEM); SEM studies using backscattered electron (BSE) images and energy dispersive X-ray spectroscopy (EDS) were performed to identify the components of the milled powders.

3. RESULTS AND DISCUSSION

As revealed in Figure 1, the homogenized sample's microstructure exhibits an equiaxed grain structure with an average grain size of 80 μm. This study used the alloy C-103, whose chemical composition is shown in Table 1.

Figure 2 shows the alloy's compressive true stress-true strain curves at different temperatures and strain rates. As can be seen, the flow behavior of alloys strongly depends on deformation temperature and strain rate. It should be noted that no correction was made on the curves because of the relatively low strain rates (below 1 s⁻¹) used in compression tests and, consequently, low

adiabatic heating. According to the curves presented in Figure 2, flow stress increases with strain at low temperatures and strain rates (e.g., 700°C and 0.001 s⁻¹) due to strain hardening created in the sample.
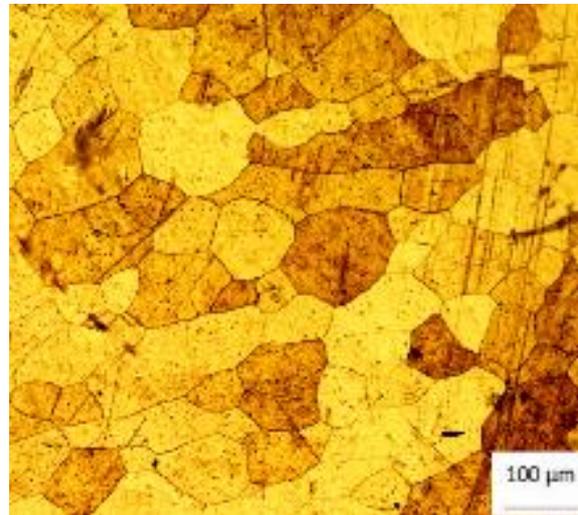

Fig. 1. Light optical microstructure of C-103 before compression test.

This behavior is also observed at 900°C and low strain rates. For the temperature of 900°C, a softening phenomenon is observed at a high strain rate of 0.4 s⁻¹ compared to the strain rate of 0.001 s⁻¹. This can be attributed to the restoration phenomena. At lower strain rates, there is a decrease in dislocation accumulation, which may not be sufficient to initiate the formation of new grains through dynamic recrystallization (DRX). Instead, dynamic recovery (DRV) may become the dominant restoration mechanism. DRV involves the elimination of dislocations through processes such as cross-slip and climb, resulting in a reduction of dislocation density without forming new grains. At a strain rate of 0.01 s⁻¹ and a temperature of 900°C, the interplay between strain rate, temperature, and solute atom mobility in the Nb alloy C103 favors dynamic recovery over dynamic recrystallization.

Figure 3 shows the variation of flow stress against temperature for different strain rates.

Table 1. Chemical composition (wt.%) of the present alloy in comparison with its standard counterpart alloy

Alloy	Nb	Hf	Ti	Zr	Ta	W	N	O	C	H
Present alloy	balance	9.5	1.25	≤0.1 ppm	≤0.1 ppm	≤0.1 ppm	1200 ppm	450 ppm	-	10 ppm
ASTM B654	balance	9-11	0.7-1.3	≤0.700	≤0.500	≤0.500	≤0.010	≤0.025	≤0.015	≤0.0015

[Downloaded from food.iust.ac.ir on 2026-02-21]   [DOI: 10.22068/ijmse.3590]
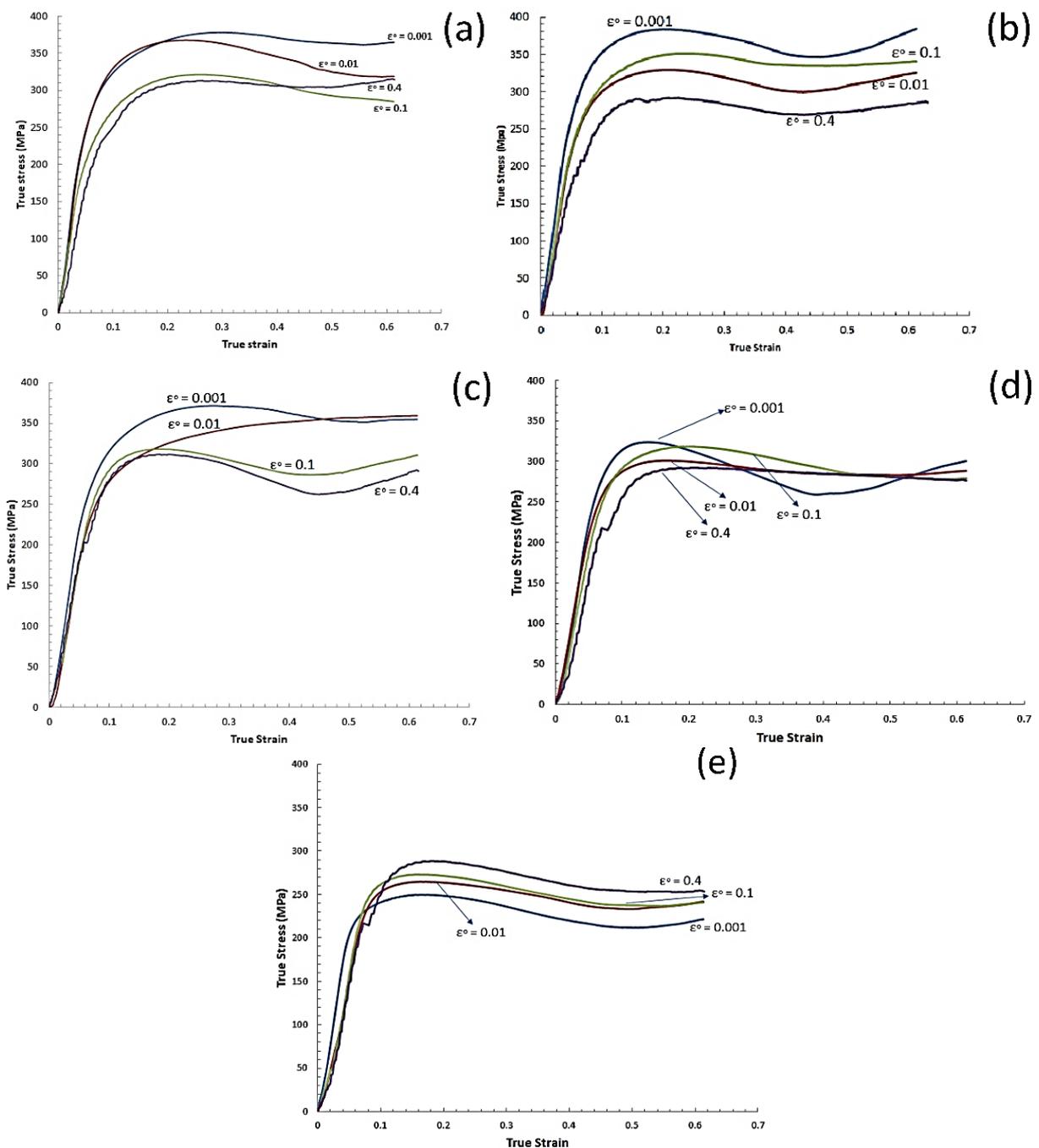
Fig. 2. Compressive stress-strain curves of C-103 at different strain rates at a) 700, b) 800, c) 900°C d) 1000°C e) 1100°C.

According to this figure, a significant decrease in flow stress is observed with increasing temperatures beyond 900°C, indicating that restoration phenomena are probably happening at temperatures higher than 900°C and low strain rates. This effect of temperature on flow stress is reduced by increasing the strain rate.

Up to 900°C, erratic manners (ups and downs) of flow stress can be seen in Figure 3. It indicates that the strain rate sensitivity coefficient is negative and varies with temperature. The proximity of stresses at a temperature of 1000°C suggests that the strain rate sensitivity coefficient is almost zero. The decreasing trend of the flow stress decreases as the strain rate increases.

It is well known that two types of restoration phenomena, including dynamic recovery (DRV) and dynamic recrystallization (DRX), can occur

during the hot deformation of alloys.
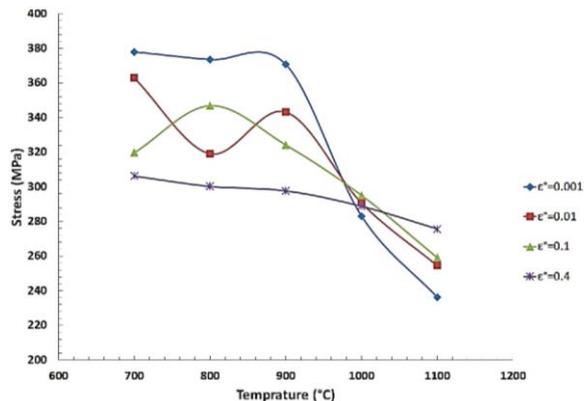
Fig. 3. Variation of flow stress with the temperature at different strain rates.

As a result of DRV, rearrangement and annihilation of dislocations take place. DRV can be identified from the stress-strain curve as a plateau region after a slight strain hardening [10]. Figure 2(a, b) stress-strain curves show that dynamic recovery occurs. The dynamic recovery phenomenon occurred in the samples at 700, 800°C, and 900°C at a low strain rate. DRV at low temperatures and low strain rates is a restoration phenomenon in high stacking fault energy materials, like Nb-based alloys. As can be seen from the stress-strain curve of the sample deformed at a temperature of 900°C and strain rates of 0.1 and 0.4 s^{-1} (Figure 2b) and also at higher temperatures (Figure 2 d,e), the flow stress increases up to a maximum and then decreases to a stable value. This behavior is commonly observed in materials showing DRX. During DRX, the flow stress initially increases to a maximum value due to strain hardening, and then it is reduced to a constant value due to restoration phenomena. There is a critical strain value at which free dislocations are created to form an initial core of dynamic recrystallization. Subsequently, softening is observed due to dislocation annihilation and the formation of several large dislocation-free regions, decreasing flow stress [10]. DRX has already been observed in pure Nb [8] and other Nb alloys such as Nb-1Zr-0.1C [10].

Another important parameter from a hot compression test is the strain rate sensitivity, calculated from the following equation for a given temperature and strain.

$$m = \frac{\partial ln\sigma}{\partial ln\dot{\varepsilon}} \qquad (1)$$

The m value is calculated from the slope of lnσ- ln($\dot{\varepsilon}$) curve at a constant temperature. Figure 4 represents the m value for different temperatures. The absolute values of m decrease as temperature increases within the 700-900°C range but then increase significantly beyond 900°C. This shows that the condition is better for hot working with increasing temperature.
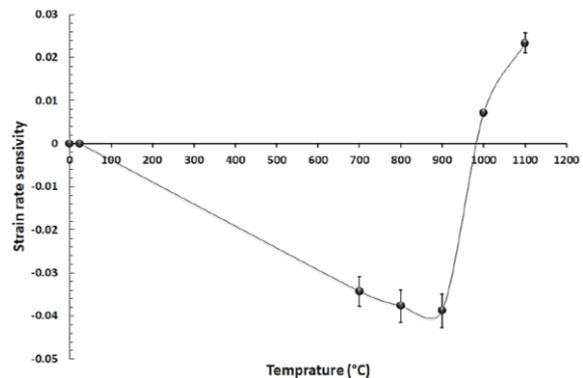
**Fig. 4.** Strain rate sensitivity of C-103 at different temperatures.

Notably, the strain rate sensitivity exhibits a negative value up to a temperature of 900°C. This means that dynamic strain aging (DSA) takes place. During DSA, there is competition between the dislocations pinned by solute atoms and free dislocations, resulting in a serration in the alloy's tensile stress-strain curve. DSA is affected by temperature and strain rate. The ability of solute atoms to diffuse to dislocations increases with increasing temperature.

Hot compression results and the curve shown in Figure 4 indicate that the strain rate sensitivity has a negative value up to 950°C. DSA results in high strength, reduced workability and surface quality of the sample, and, in some cases, cracking. Similar results have been reported in pure Nb and its other alloys [11]. For example, commercially pure Nb exhibits the DSA at 300–500°C [12,13]. Park et al. [14] A likely mechanism for DSA in CP-Nb was suggested. Sheely [15] has also studied the compressive properties of CP-Nb up to 1200°C and showed that the effect of DSA is lost beyond 700°C. Panwar et al. [11] have studied the tensile properties of the C-103 alloy at the temperature range of 25-1200°C. They showed that the serrations in corresponding stress-strain curves are attributed to DSA in C-103. DSA dominates in the 600-900°C range, while oxidation and dynamic recovery control

tensile properties at high temperatures.

According to Figure 4, in the temperature range of 700-900°C, where the m value is negative, instability in plastic deformation (i.e., local deformation) occurs as a result of adiabatic heating. Localized deformation can be observed as shear bands or dead zones in the specimen and machine contact area. On the other hand, DRX takes place in the range of 1000-1100°C, and the strain hardening rate increases significantly. The strain hardening rate is determined by $\gamma = \frac{1}{\sigma} \left(\frac{d\sigma}{d\varepsilon}\right)|_{\varepsilon}$ which is converted to the equation of $\gamma = \frac{1}{\sigma_i} \frac{\sigma_{i+1}-\sigma_{i-1}}{\varepsilon_{i+1}-\varepsilon_{i-1}}$ using the numerical differentiation method. Flow localization parameter (FLP) is introduced to predict the strain localization and formation of shear bands and consequently to estimate workability [16]. This parameter is defined as $FLP = \frac{\gamma-1}{m}$. If FLP is positive, plastic instability would be possible, and when FLP is higher than

5, severe deformation localization occurs [16]. In this regard, the FLP of C-103 was calculated to be +30 for deformation to a strain of 0.6 at a temperature of 700°C and strain rate of 0.4 s⁻¹. This is a very high value for FLP showing strain localization in the mentioned deformation condition. Figure 5 shows the corresponding specimen and its microstructure after deformation at this condition. Some cracks were observed on the surface of the sample. The sample's microstructure shown in Figure 5b also observes locally deformed areas. The average grain size in Figure 5 is 20 µm.

According to Figure 3, the m value is positive at 1100°C, so strain localization is expected not to be observed, and hot deformation of the sample will be performed easily. The occurrence of DRX is identified from the microstructure shown in Figure 6, which may lead to enhanced workability. It should be mentioned that the oxidation of C-103 severely takes place at 1100°C, as shown in Figure 6.
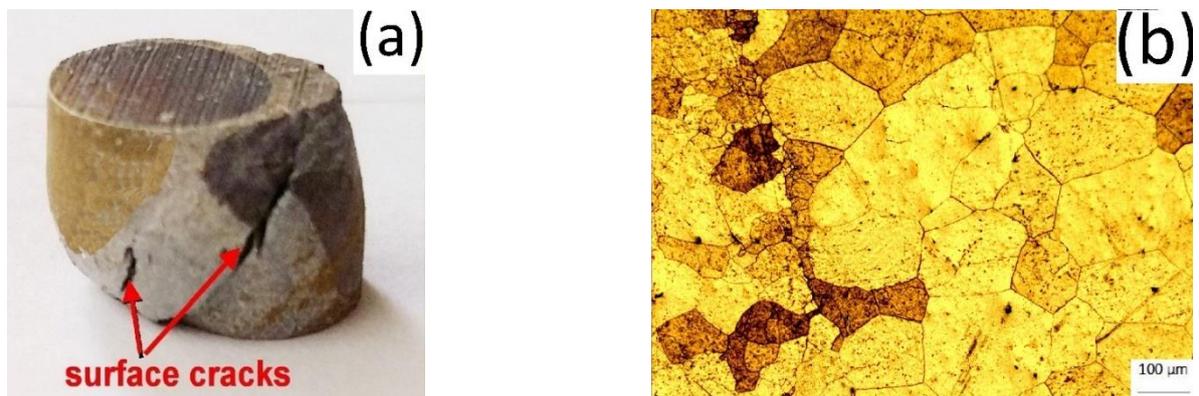
Fig. 5. a) the sample deformed at 700°C and strain rate of 0.4 s⁻¹ and b) corresponding light optical microstructure.
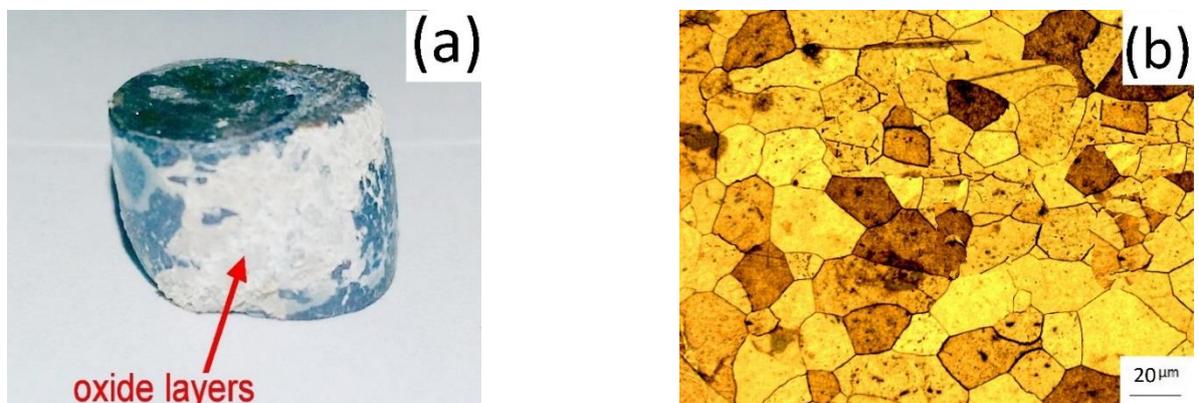
Fig. 6. a) the sample deformed at 1100°C and strain rate of 0.4 s⁻¹ and b) corresponding light optical microstructure.

5

H. Momeni et al.

It can be said that inhomogeneous deformation does not occur during deformation at a temperature of 1100°C, and the strain rate is 0.4 s^{-1} to a true strain of 0.3, at which restoration phenomena such as DRX take place and average grain size of almost 5μm. FLP also confirms this, as it was calculated to be -69 in the corresponding deformation condition.

Hafnium is more likely to oxidize than niobium. So, hafnium oxide begins to form in the grain boundary. Figure 7 shows the microstructure of samples after hot compression tests.

The Formation of HfO$_2$ precipitates and oxidation can cause brittleness of C-103 alloy at high temperatures. Figure 8 shows the sample's microstructure deformed at 900°C and the strain rate of 0.1 s^{-1}.

As can be seen, discontinuous dynamic recrystallization (dDRX) with an average grain size of 33 μm occurred in this sample. Figure 8 shows the regions of recrystallized grains along with other grains.
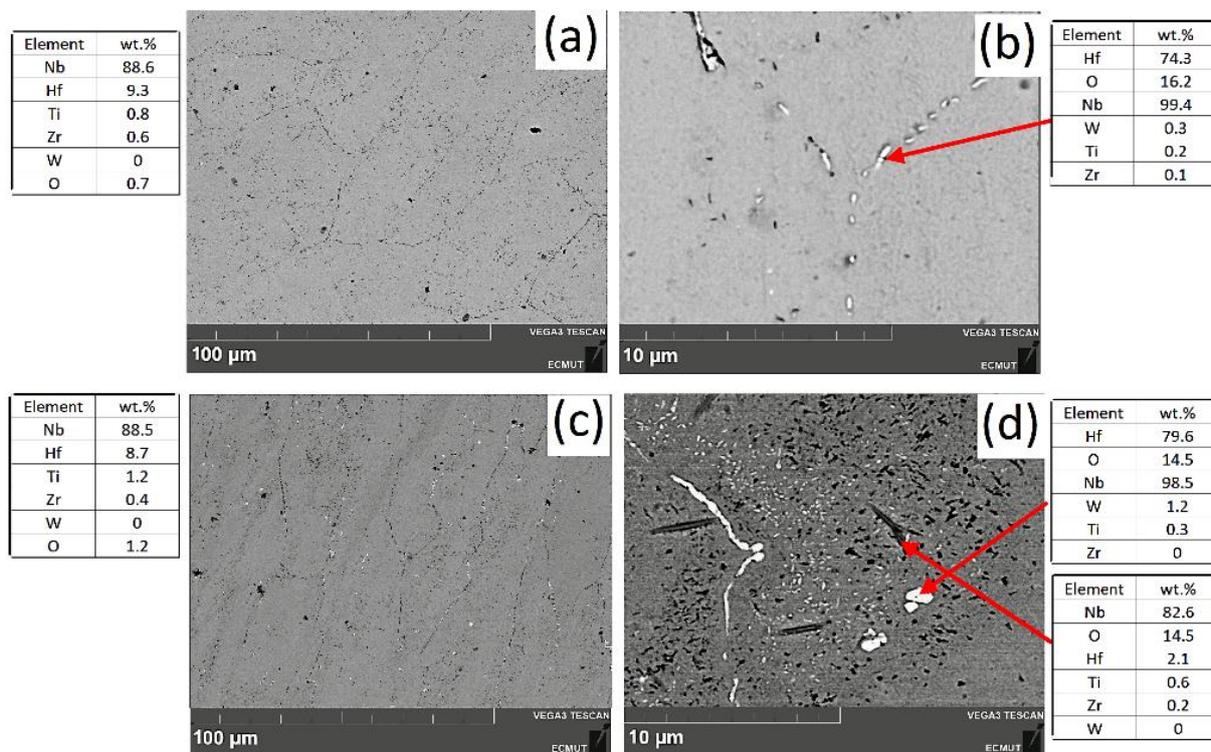

Element	wt.%
Nb	88.6
Hf	9.3
Ti	0.8
Zr	0.6
W	0
O	0.7

Element	wt.%
Hf	74.3
O	16.2
Nb	99.4
W	0.3
Ti	0.2
Zr	0.1

Element	wt.%
Nb	88.5
Hf	8.7
Ti	1.2
Zr	0.4
W	0
O	1.2

Element	wt.%
Hf	79.6
O	14.5
Nb	98.5
W	1.2
Ti	0.3
Zr	0

Element	wt.%
Nb	82.6
O	14.5
Hf	2.1
Ti	0.6
Zr	0.2
W	0

Fig. 7. SEM images of microstructure of samples after hot compression test at a, b) 900°C and c, d) 1100°C
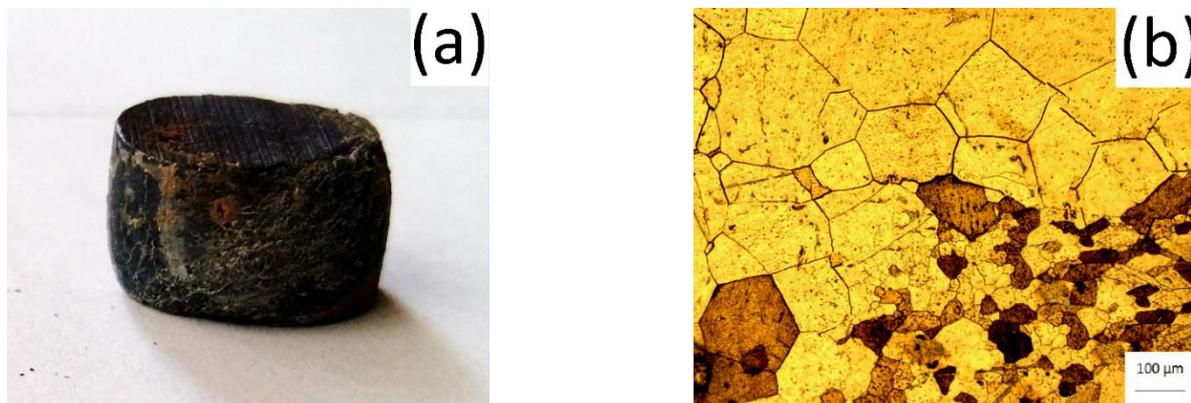

Fig. 8. a) The sample deformed at 900°C and strain rate of 0.1 s^{-1} and b) corresponding light optical microstructure.

Given that severe oxidation is observed at high temperatures such as 1100°C and localized deformation and dynamic strain aging occur in the range of 700-900°C, it is concluded that the temperature range of 950-1000°C and strain rate of 0.001-0.1 s⁻¹ can be the suitable condition for hot deformation of C-103. At temperatures where deformation and thermally activated restoration phenomena occur, the microstructure is affected by strain temperature and strain rate. Both strain rate and deformation temperature are considered by the Zener-Hollomon equation as follows:

$$Z = \dot{\varepsilon} exp(\frac{Q}{RT}) = A(sinh(\alpha\sigma))^n \qquad (2)$$

R is the gas constant, and Q is the apparent activation energy for plastic flow. Understanding the relationship between flow stress, strain, temperature, and strain rate is a prerequisite to interpreting and modelling the hot deformation behavior. Suppose the flow stress follows a mechanical state equation dependent on the transient values of T, ε, and script epsilon dot. In that case, a simple experimentally obtained equation can describe the relationship between these parameters. It has been demonstrated that during hot deformation at a steady state, the relationship between the flow stress and Z is as follows:

$$Z = c_1(sinh(c_2\sigma))^n \qquad (3)$$

where c_1, c_2, and n are equation constants. The Equation (3) can also be written as follows:

$$\sigma = \frac{1}{c_2} ln\left[\left(\frac{Z}{c_1}\right)^{1/n} + \left(\left(\frac{Z}{c_1}\right)^{2/n} + 1\right)^{1/2}\right] \qquad (4)$$

Z strongly correlates with flow stress and, consequently, with dislocation density. Z parameter is suitable for studying the hot deformation process at which temperature and strain rate are given, but flow stress cannot be measured directly.

Equations 2-4 were used in this study to estimate the hot deformation behavior of C-103. The constants of the equations were determined from the results of uniaxial hot compression tests. In these equations, A, n, and α are coefficients obtained from the Zener-Hollomon equation. The following equation is obtained by differentiating from the Zener-Hollomon equation.

$$ln(\dot{\varepsilon}) + \frac{Q}{RT} = n * ln\, sinh(\alpha\sigma) + lnA \qquad (5)$$

In a constant temperature, n and α can be determined by drawing $ln(\dot{\varepsilon})$ against $ln\, sinh(\alpha\sigma)$ for different strains and steady-state stress of the flow curve. To determine these coefficients, an initial value (e.g., 0.01) is considered for α; then its value is changed so that all plotted lines for different temperatures are parallel. Usually, a value between 0.02 and 0.08 MPa⁻¹ is chosen for α, and then the best-fit coefficient is selected as the α coefficient. The slope of the line passing the points and its intercept with the y-axis determine n and lnA, respectively. It is worth mentioning that the average value is usually reported due to the decrease of the n value with increasing temperature. To determine the Q value in Equation 6, the variation of ln sinh (ασ) versus 1/τ is plotted. It should be mentioned that due to the negative value of m, temperatures at which the m value is positive were used.

$$Q = -R\frac{\partial \, ln(\dot{\varepsilon})}{\partial \, ln\left(\frac{1}{T}\right)} = -8.314 \times -32160 \qquad (6)$$

The constants of Equation 1, showing the flow behavior of C-103, were measured as listed in Table 2.

These values for Nb and its other alloys are also listed in Table 2. The calculated value for Q is close to the activation energy of Nb and is lower than the activation energy for the self-diffusion of Nb (Q= 400 kJ/mol) [17]. The apparent activation energy (Q= 2/3Q_SD) considers other concurrent physical phenomena, such as recovery. This explains why Q differs from niobium's bulk diffusion (QSD) coefficient. The effect of grain boundary diffusion becomes relevant in nanostructured materials, and it can be neglected in coarse-grained materials like the samples that VAR produces.

Table 2. The constants of the Zener-Hollomon equation obtained for C-103 in comparison with pure Nb and its other alloys.

Material	n	$\alpha\,(\frac{1}{MPa})$	Q (KJ/mol)	Ref.
Nb-10Hf-1Ti (C-103)	13.9	0.01	267	This work
Nb	7.5	0.001	246	[8]
Nb-1Zr-0.1C	5	-	361	[10]
Nb-1Zr	4.9	0.02	259	[19]

If n >3, the dominant deformation mechanism is the dislocation-base mechanism. Nieh et al. [18] showed that the n value at 1100°C is about 14.8 for Nb-1Zr alloy due to the power-law breakdown regime. The Equation 1 for C-103 was calculated to be as follows:

$$CapZ = \dot{\varepsilon} \exp\left(\frac{267.380}{RT}\right) = 595.87(sinh(0.01\sigma))^{13.9}$$

(7)

Equation 7 calculates the flow stress of C-103 at different temperatures and strain rates, which would help design appropriate forming processes.

4. CONCLUSIONS

In the present study, the hot deformation behavior of C-103 has been investigated in the temperature range of 700-1100°C and the strain rate range of 0.001-0.4 s^{-1}. From the compressive flow curves, microstructure evolutions, and constitutive analysis, the following conclusions have been drawn:

1. The strain rate sensitivity was almost constant and showed a negative value in the temperature range of 700-900°C but increased significantly beyond 900°C.
2. In the temperature range of 700-900°C, local deformation and dynamic strain aging were observed, and dynamic recovery at low temperatures and low strain rate was a restoration phenomenon. While dDRX occurred in the 900-1100°C range, the strain hardening rate increased significantly.
3. Severe oxidation occurred in the temperature range of 1000-1100°C, and localized deformation and dynamic strain aging occurred in the 700-900°C range. Therefore, the ranges of 950-1000°C and 0.001-0.1 s^{-1} were suggested to be suitable conditions for hot deformation of C-103.
4. In the studied domain, the strain rate sensitivity varied from -0.04 to 0.02, the stress exponent was 13.9, and the activation energy of deformation was obtained as 267 kJ/mol.
5. The constitutive equation of C-103 for hot deformation was determined to be $Z = 595.87(sinh(0.01\sigma))^{13.9}$.

REFERENCES

[1]. Sheftel EN, Bannykh OA. "Niobium-Base alloys", Int J Refract Met Hard Mater 1994; 12, 303–14. https://doi.org/10.1016/0263-4368(93)90038-H.

[2]. Committee ASMH. Properties and Selection: "Nonferrous Alloys and Special-Purpose Materials.", ASM International; 1990. https://doi.org/10.31399/asm.hb.v02.9781 627081627.

[3]. Chang W. "C-103 Niobium Properties and Products", 2010, 1–27.

[4]. Nemat-Nasser S, Guo W. "Flow stress of commercially pure niobium over a broad range of temperatures and strain rates", Mater Sci Eng A, 2002; 284: 202–10. https://doi.org/10.1016/s0921-5093(00)00740-1.

[5]. Kiessig H, Essmann U. "Flow stress of pure niobium between 2200 K and the melting point 2741", K. Scr Metall 1985;19,989–92. https://doi.org/10.1016/0036-9748(85)90297-2.

[6]. Sha J, Hirai H, Tabaru T, Kitahara A, Ueno H, Hanada S. "High-temperature strength and room-temperature toughness of Nb–W–Si–B alloys prepared by arc-melting.", Mater Sci Eng A 2004; 364, 151–8. https://doi.org/10.1016/j.msea.2003.08.014.

[7]. Chou I, Koss DA, Howell PR, Ramani AS. "High-temperature deformation of a mechanically alloyed niobium-yttria alloy.", Mater Sci Eng A 1997; 222; 14–20. https://doi.org/10.1016/S0921-5093(96)10450-0.

[8]. Behera a. N, Kapoor R, Sarkar a., Chakravartty JK. "Hot deformation behaviour of niobium in temperature range 700–1500°C." Mater Sci Technol, 2014; 30, 637–44. https://doi.org/10.1179/1743284713Y.000 0000387.

[9]. Sankar M, Reddy YS, Baligidad RG. "Effect of different thermomechanical processing on structure and mechanical properties of electron beam melted niobium." Trans Indian Inst Met 2009; 62, 135–9. https://doi.org/10.1007/s12666-009-0018-9.

[10]. Sarkar a., Kapoor R, Verma a., Chakravartty JK, Suri a. K. "Hot deformation behavior of Nb–1Zr–0.1C alloy in the temperature range 700–1700°C." J Nucl Mater, 2012, 422, 1–7.

https://doi.org/10.1016/j.jnucmat.2011.11.064.

[11]. Panwar SS, Prasad K, Umasankar Patro T, Balasubramanian K, Venkataraman B. "On the occurrence of dynamic strain aging in C-103 Nb based alloy." Mater Sci Eng A, 2014; 620, 286–92. https://doi.org/10.1016/j.msea.2014.10.016.

[12]. Sankar M, Baligidad RG, Gokhale AA. "Effect of oxygen on microstructure and mechanical properties of niobium." Mater Sci Eng A, 2013; 569, 132–6. https://doi.org/10.1016/j.msea.2013.01.025.

[13]. Szkopiak ZC, Miodownik AP. "The mechanism of strain-ageing in commercially pure niobium." J Nucl Mater 1965; 17, 20–9. https://doi.org/10.1016/0022-3115(65)90143-1.

[14]. Park SC, Beckerman LP, Reed-hill RE. "On the Portevin-Le Chatelier Effect Due to Snoek Strain Aging in the Niobium Oxygen System." Metall Trans A 1983; 14, 463–9. https://doi.org/10.1007/bf02644223.

[15]. Sheely WF. "Mechanical properties of niobium-oxygen alloys." J Less Common Met, 1962; 4, 487–95. https://doi.org/10.1016/0022-5088(62)90036-X.

[16]. Dieter GE, Kuhn H a, Semiatin SL. "Handbook of Workability and process design." ASM Int 2003,280.

[17]. Atkins AG. "Deformation-mechanism maps the plasticity and creep of metals and ceramics". J Mech Work Technol, 1984, 9, 224–5. https://doi.org/10.1016/0378-3804(84)90015-9.

[18]. Nieh TG, Zhang M, Zinkle SJ, McGreevy TE, Hoelzer DT, Speakman S a. "Effect of texture on the high temperature mechanical properties of Nb–1%Zr alloy.", Scr Mater 2006; 55, 719–22. https://doi.org/10.1016/j.scriptamat.2006.06.025.

[19]. Behera AN, Chaudhuri A, Kapoor R, Chakravartty JK, Suwas S. "High temperature deformation behavior of Nb-1wt.%Zr alloy." Mater Des 2016, 92, 750–9. https://doi.org/10.1016/j.matdes.2015.12.077.